ORIGINAL ARTICLE

Multiamine-induced self-healing poly (Acrylic Acid) hydrogels with shape memory behavior

Jun Lan[1] · Xiuquan Ni[1] · Chuanzhuang Zhao[1] · Qiao Liu[2] · Chongyi Chen[1]

Abstract

In this work, a versatile and simple strategy for building self-healing hydrogels with tunable mechanical properties and shape memory behavior is reported. A commercially available small molecule with three amino groups, diethylenetriamine (DETA), is applied to crosslink poly (acrylic acid) (PAAc) chains via ionic bonding, and the complexes of the PAAc chains with DETA form hydrophobic microdomains in the hydrogel network. The cooperation of ionic bonding and hydrophobic interactions drastically improves the mechanical properties, which can be modulated by adjusting the molar ratio of PAAc to DETA. Due to the physical interaction of the crosslinks, the hydrogels can self-heal rapidly in ambient conditions. The thermal responsiveness of the physical microdomain crosslinks endow the hydrogels with shape memory behavior. It is hoped that this novel strategy will provide new opportunities for the design of high-strength hydrogels with variable functionalities for a wide range of applications, such as artificial muscle and skin.

Introduction

Self-healing is an important feature of biological systems, and the self-healing ability of biological materials involves sacrificial bonds that break and reform dynamically through an energy dissipation mechanism before fracture of the molecular backbone [1–3]. Self-healing hydrogels are able to restore their initial properties after the formation of interior or exterior cracks, which is similar to the behavior of some living materials, such as human skin and muscles [4–7]. Although traditional hydrogels exhibit superior performance, their desirable properties and the integrity of their network structure deteriorate when the materials suffer microscale or macroscale injury, which limits their lifetime.

Various kinds of self-healing hydrogels have been designed for diverse applications, such as biosensors [8], drug delivery systems [9], and wound healing [10]. Self-healing hydrogels are always crosslinked by dynamic bonding through reversible molecular interactions, such as

hydrogen bonding [11, 12], ionic bonding [13], molecular recognition [14–16], and hydrophobic associations [17]. However, the relatively poor mechanical strength and toughness of self-healing hydrogels remains a challenge, which prevents them from any stress-bearing applications such as cartilage and tissue engineering scaffolds. This limitation is because the self-healing ability of hydrogels opposes the mechanical strength and toughness. Extensive efforts have been made to improve the mechanical properties of self-healing hydrogels [18–20]. The network structures have been optimized via the introduction of multiple bonding modes [19, 21]. Hydrophobically modified PAAc chains with CTA counterions form a physical network that contains both ionic bonding and hydrophobic effects [22]. The incorporation of hydrophobic sequences within the hydrophilic polymer chains via micellar polymerization generates dynamic hydrophobic associations between the hydrophobic domains of the polymer chains and the surfactant micelles acting as physical crosslinks of the resulting

✉ Chongyi Chen
  chenchongyi@iccas.ac.cn

1 Ningbo Key Laboratory of Specialty Polymers, College of Materials Science and Chemical Engineering, Ningbo University, 315211 Ningbo, China

2 Institute of Materials, Ningbo University of Technology, Ningbo, 315016 Ningbo, China

hydrogels that play crucial roles in the crosslinked network; therefore, the self-healing hydrogels exhibit high mechanical strength. On the other hand, most self-healing systems usually require either sophisticated synthesis of the polymers, the encapsulation of healing agents or variations in the ambient conditions, such as the pH or temperature.

In this work, we selected a small molecule, diethylenetriamine (DETA), which contains two primary and one secondary amino groups, as a crosslinking agent. A simple strategy was presented for the preparation of self-healing hydrogels via ionic bonding and hydrophobic interactions by introducing the multiamine into the PAAc network in situ. The hydrogels could self-heal rapidly without the need for human intervention or external energy. Reversible physical microdomain associations endowed the hydrogels with shape memory behavior and a repeatable high shape-fixing efficiency.

Materials and methods

Materials

Unless otherwise noted, all commercial reagents were used as received including diethylenetriamine (DETA) (>99%, Aladdin Chemical, Shanghai, China), acrylic acid (AAc) (>99%, Aladdin Chemical, Shanghai, China), and ammonium persulfate (APS) (>99%, Aladdin Chemical, Shanghai, China).

Typical preparation of hydrogels

An acrylic acid (0.07 mol, 5.0 g) aqueous solution (20 mL) was continuously stirred in an ice water bath, and DETA (0.0116 mol, 1.19 g) was slowly added into the solution. Then, ammonium persulfate (APS) (0.05 g) was added to the mixture. This mixed transparent solution was transferred to a 1-ml plastic syringe (diameter = 4.6 mm), and a white, soft PAAc/DETA hydrogel formed after reaction for 6 h at 60 °C. Different molds were used to prepare hydrogels with different shapes. The as-prepared PAAc/DETA hydrogels were treated by dialysis for 3 days to obtain virgin hydrogels.

Chemical characterization

Fourier transform infrared (FT-IR) spectra of all samples were taken using a Nicolet 460 IR spectrometer. All samples were examined in pressed KBr pellets in which the dry hydrogel and polymer powder were mixed with KBr in a weight ratio of 0.5–1%. ^{1}H NMR measurements were carried out on a Bruker AVANCE II 400 MHz NMR spectrometer using D_2O as the solvent.

Rheological experiments

The rheological properties were monitored by frequency sweep, strain sweep, and temperature sweep experiments by using a rotational rheometer (ARES-G2, TA Instruments, USA) with a hatched plate 25 mm in diameter. A PAAc/DETA hydrogel sheet with a thickness of 2 mm was cut into a circle 25 mm in diameter and then put on the bottom plate of the rheometer for the frequency and strain sweep measurements at 25 °C. Temperature sweep experiments were performed with a heating rate of 0.33 °C/min. For both the time and temperature sweep experiments, a constant strain of 10% and a frequency of 1 Hz were used.

Tensile tests

The hydrogel tensile test was performed on a Shenzhen Kaiqiangli Testing Instruments KD III-0.05 tensile testing machine. All hydrogel samples with a diameter of 4.6 mm were tested with a crosshead speed of 50 mm·min^{-1} at 25 °C. The engineering tensile stress (σ) was calculated as $\sigma = L/(\pi R^2)$, where L is the load and R is the original radius of the specimen. The engineering tensile strain (ε) was defined as the change in length (l) relative to the initial gauge length (l_0) of the specimen, $\varepsilon = l/l_0 \times 100\%$. The initial modulus ($E$) was calculated as the slope of the stress−strain curve within the range $\varepsilon = 50 - 100\%$. The fracture toughness was characterized by the fracture energy, which was calculated by integrating the area under the stress−strain curve. In the cyclic tensile test of the PAA-D-n hydrogel, both loading and unloading were performed at a constant velocity of 50 mm·min^{-1}. The waiting time was the recovery time from the end of the first cycle to the second cycle stretch. In the hysteresis measurement, a dumbbell-shaped sample was first stretched to a predetermined stretch ratio and then unloaded to zero force at the same velocity of 50 mm·min^{-1}. The dissipation energy was defined as the area under a cycle of the loading−unloading curve.

$$U = \int \sigma d\varepsilon \tag{1}$$

Swelling measurements

Lyophilized PAA-D-n hydrogel samples were immersed in large excess of deionized water at 25 °C, and the weight of the PAAc/DETA hydrogel was measured every 30 min. The equilibrium swelling ratio was calculated by the equation $Q_v = (W_s - W_d)/W_d \times 100\%$, where Ws and Wd are the weights of the swollen hydrogel and the corresponding dried gel, respectively.

Table 1 Parameters of the PAA-D-n hydrogels

Entry	AAc (mmol/mL)	DETA (mmol/mL)	ESR[a]	$\tau_\alpha = 2$[b] (kPa)	E[c] (kPa)
PAA-D-2	35	5.80	0.347	57.3	0.76 ± 0.05
PAA-D-3	35	3.85	1.270	58.1	0.79 ± 0.06
PAA-D-4	35	2.90	1.208	61.9	0.85 ± 0.04
PAA-D-5	35	2.30	1.067	51.3	0.76 ± 0.07
PAA-D-6	35	1.95	1.010	46.8	0.68 ± 0.04
PAA-D-7	35	1.75	1.469	30.3	0.42 ± 0.03

[a]Equilibrium swelling ratio

[b]Stress at 100% strain

[c]Elastic modulus within the range $\varepsilon = 50\text{--}100\%$
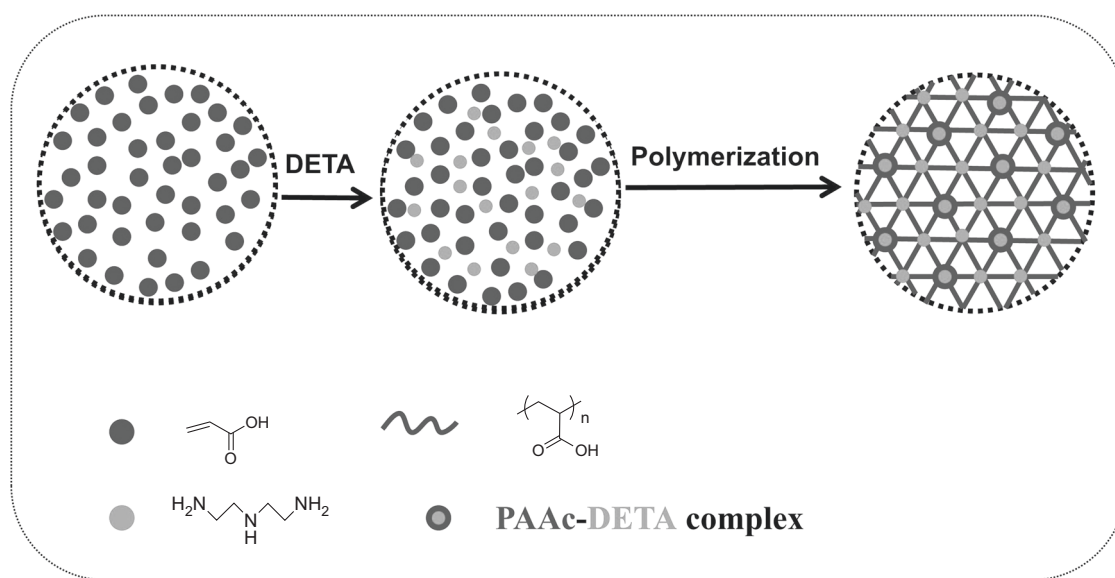
Scheme 1 Schematic illustration of the preparation of PAAc/DETA hydrogels

Self-healing behavior measurements

Virgin hydrogel samples 4.6 mm in diameter and 6 cm in length were cut in the middle, and then the two halves were brought into contact within a plastic syringe (of the same diameter as the gel sample) by slightly pressing the piston plunger. The hydrogel samples were healed at room temperature for 1 day and then subjected to dialysis for 3 days in deionized water to realize healing of the hydrogels.

Shape-fixing efficiency measurements

Cylindrical gel samples were immersed in a water bath at 60 °C. The gels became soft and were stretched at 60 °C to twice their original lengths. Then, the temporary shapes were fixed by immersing the gel samples in a water bath at 25 °C for 1 min. The shape-fixing efficiency, F, which represents the ability of the gel sample to hold its temporary shape, was calculated as follows [23]: $F = (l_t - l_0)/(l_s - l_0)$, where l_0 and ls are the initial and stretched lengths of the gel sample, respectively, and l_t is the sample length after a fixing time of $t = 1$ min at 25 °C. The interval time for each shape-fixing experiment was 2 min.

Results and discussion

Formation mechanism of the PAA-D-n hydrogels

The PAAc/DETA hydrogels were synthesized via in situ free radical polymerization of acrylic acid (AAc) in an aqueous diethylenetriamine (DETA) solution, and all the hydrogels were opaque, indicating the formation of a two-phase structure. The as-prepared PAAc/DETA hydrogels were treated by dialysis for 3 days to obtain virgin hydrogels. By

Fig. 1 a FTIR spectra of DETA, PAAc and the PAA-D-n hydrogels. **b** ^{1}H NMR spectra of DETA, PAAc and the mixture of DETA and PAAc before and after heating
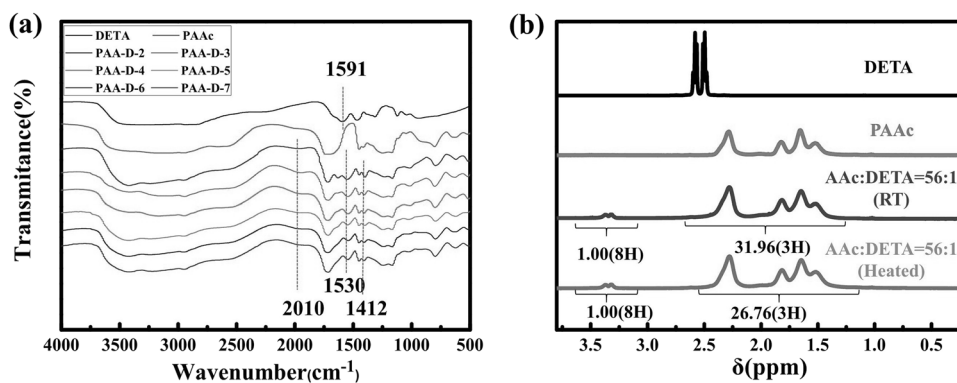

Fig. 2 a Tensile stress–strain curves of the virgin PAA-D-n hydrogels. **b** Work of extension at fracture of the virgin PAA-D-n hydrogels. **c** Swelling behavior of the virgin PAA-D-n hydrogels in deionized water. **d** Tensile stress–strain curves for the as-prepared and virgin PAA-D-3 hydrogels
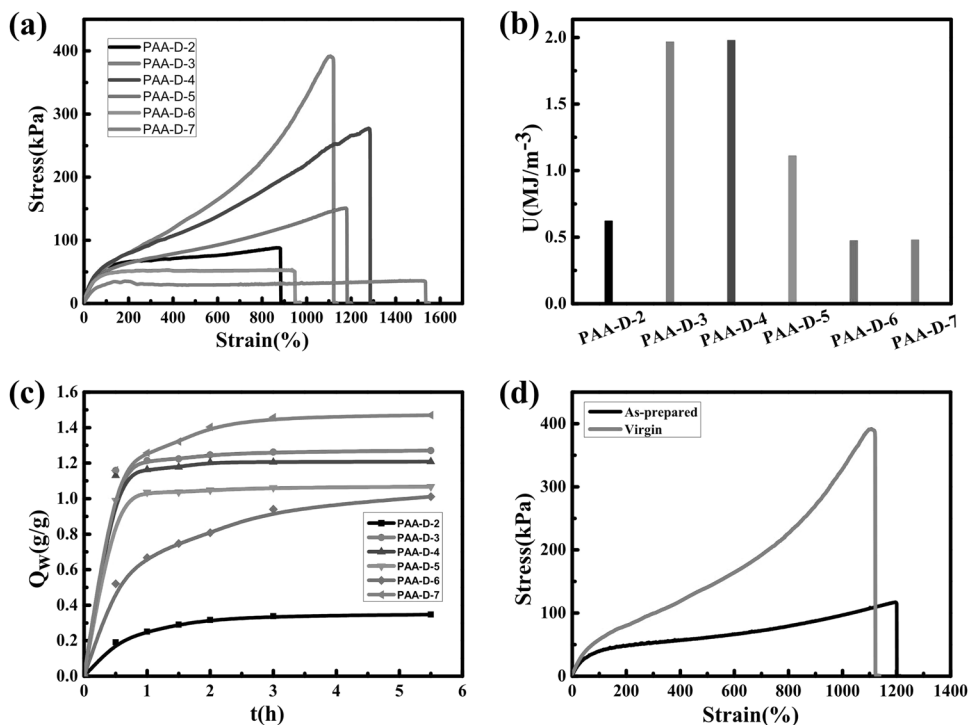
immersing the as-prepared hydrogels in water, small counterions and impurities were removed, and DETA could form more adequate ionic bonds with PAAc. The parameters and preparation of the virgin PAAc/DETA hydrogels are shown in Table 1 and Scheme 1. The samples are referred to as PAA-D-n, where D is the abbreviation for DETA and n is the ratio of carboxyl groups on PAAc to amino groups on DETA. The formation of ionic bonds between the carboxylic acid groups and amino groups was further confirmed by FTIR (Fig. 1a). The NH$_2$ band of DETA at 1591 cm^{-1} shifted to the stretching band of NH$_3^+$ at 2010 cm^{-1} in the PAA-D-n hydrogels [24, 25]. Meanwhile, the bands at 1530 and 1412 cm^{-1} were attributed to deformation of the primary/secondary ammonium ions and of the secondary ammonium ions, respectively [24]. These results suggest the formation of ionic bonds between the carboxylic acid groups and amino

groups. Figure 1b shows the NMR spectra of DETA, PAAc and the complex of PAAc and DETA before and after heating. The signal for CH_2–CH_2 in DETA appeared at 2.54 p.p.m. and moved to 3.35 p.p.m. after the formation of ionic bonds with PAAc. The feed ratio of AAc repeating units to DETA was 56:1; however, the molar ratio calculated from the integral ratio decreased to 85:1 after the formation of the PAAc/DETA complex. Interestingly, the integral ratio increased to 71:1 after heating the deuterated aqueous solution, which indicates that dissociation of the complex between PAAc and DETA occurred after heating, and this transition was completely reversible. Therefore, the dissociation and formation of complex can be attributed to temperature-related reversible ionic bonding.

The molar ratio of AAc to DETA plays a key role in determining the mechanical strength and stiffness of the
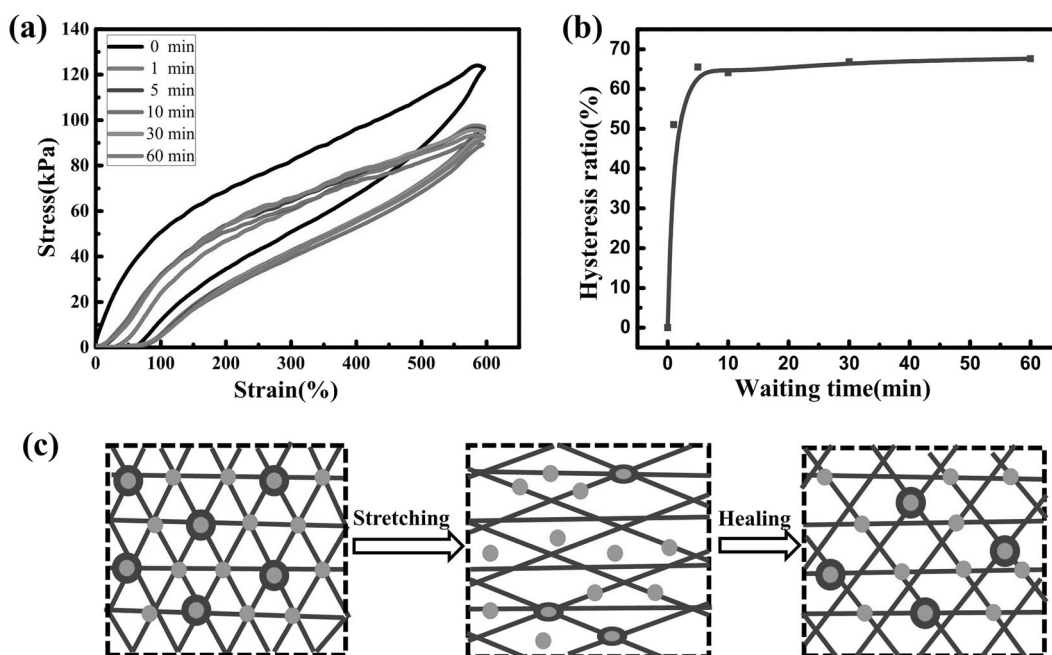
Fig. 3 a The stress–strain curve of the PAA-D-3 hydrogel for different waiting times performed by cyclic tensile tests. b Waiting time dependence of the hysteresis ratio (area ratio of the second hysteresis loop to the first). c Schematic diagram of the transition of the physical associations in the loading/unloading cycles

hydrogel. Figure 2a shows the tensile stress-strain curves for the virgin PAAc/DETA hydrogels with different molar ratios of AAc to DETA. Interestingly, for different n values, the tensile stress-strain data exhibit an unconventional trend. For $n = 2$, because of the high hydrophobic content composed of PAAc and the DETA complex, large hydrophobic domains form in the polymer chain network, and hence, an opaque hydrogel is observed. However, the high hydrophobic content increases the number of defects in the bulk hydrogel, and as a result, the fracture stress of PAA-D-2 is only 88 kPa with a fracture strain less than 900%. Unexpectedly, when we decrease the ratio of amine, the PAA-D-3 hydrogel exhibits a fracture stress of 0.4 MPa and a tensile strain of 1100%. The drastic increase in the modulus with decreasing hydrophobic content is attributed to the formation of amine-crosslinked PAAc microdomains that provide softer fillers and sacrificial bonds in the hydrogel network [26]. For $n = 4$, which corresponds to a lower ratio of amines, the fracture stress decreases and the fracture strain increases, which was expected due to the reduction in the hydrophobic interactions. However, when the content of amine is decreased even more ($n = 5$, 6), the ionic bonding and hydrophobic interactions between the polymer chains become much weaker. In comparison with microdomain macro-cross-linkers, ionic bonding becomes the main mode of cross-linking; therefore, both the fracture stress and strain decrease due to the lack of softer fillers and sacrificial bonds. When n reaches 7, the crosslinking density is even

lower, and the fracture stress decreases as a result; however, due to slippage between the polymer chains, the fracture strain increases [27]. The work of extension at fracture of the different PAAc/DETA hydrogels was calculated according to the stress-strain curves, as shown in Fig. 2b. When $n = 2$ and 3, the hydrogels exhibit the highest toughness, as these hydrogels possess the largest number of sacrificial bonds that can dissipate energy during stretching of the hydrogels.

The swelling ratio of the virgin PAAc/DETA hydrogels was measured during a period of soaking the lyophilized hydrogels in water. Figure 2c shows that the swelling ratio of the hydrogels exhibits a sudden increase during the first 1 h and reaches a stable value after 3 h. PAA-D-2 exhibits the lowest swelling ratio because of its high content of aggregated hydrophobic microdomains. However, the swelling degree sharply increases from PAA-D-2 to PAA-D-3 at first, slightly decreases from PAA-D-3 to PAA-D-6, and then increases from PAA-D-6 to PAA-D-7. This abnormal phenomenon indicates that there should be different crosslink types for the different amine contents, which is caused by two competing factors: the degree of ionization and the crosslink density [28, 29]. For n values within the range from 3 to 6, the separated hydrophobic microdomains dissociate after soaking in water, and the swelling degree decreases with the reduction in the number of carboxylate and ammonium ions. When n increases from 6 to 7, the drastic increase in the swelling degree can be attributed to the lower crosslink density.
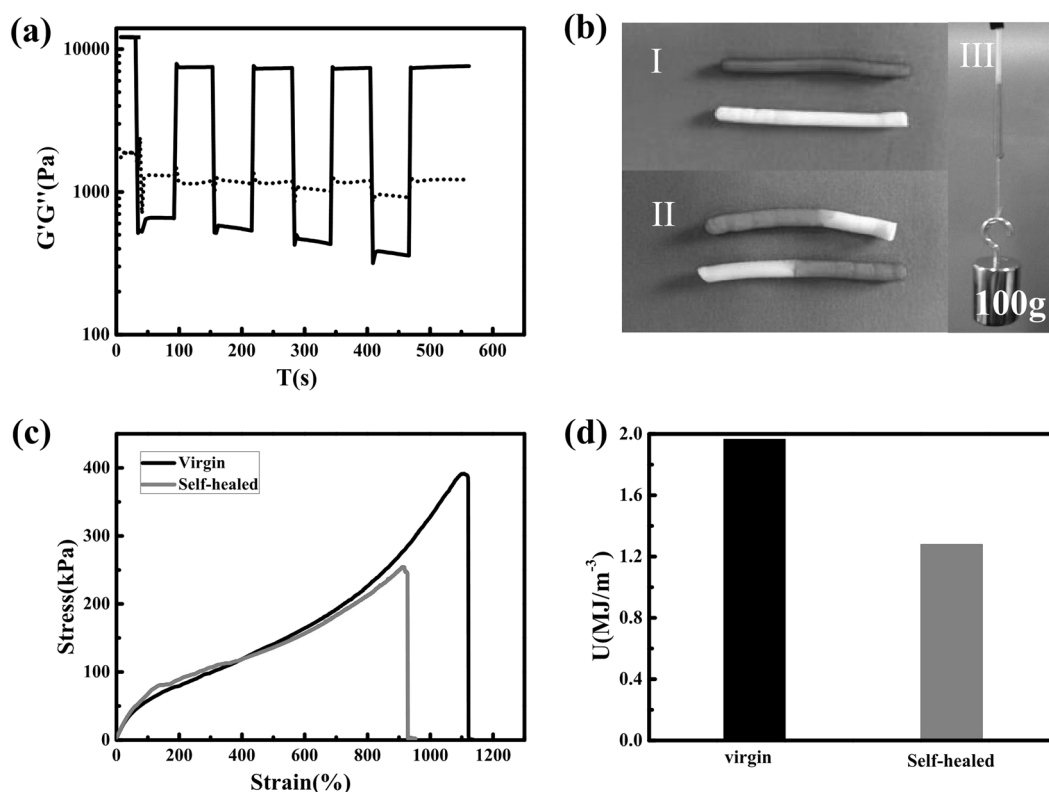
Fig. 4 a G′ (solid line) and G″ (dotted line) of the PAA-D-3 hydrogel in continuous step shear measurements (25 °C). Large strain (10) inverted the G′ and G″ values to give the sol state. On the other hand, G′ was recovered under a small strain (0.1) within 60 s. **b**, I: Two pieces of virgin PAA-D-3 hydrogel, one of which was dyed with rhodamine; II: the self-healed samples after 24 h of healing time; III: photograph demonstrating the large deformation of the self-healed samples. **c** Stress–strain curves of the virgin and self-healed bulk samples. **d** Toughness of the virgin and self-healed PAA-D-3 hydrogels

The stress–strain curves of the as-prepared PAA-D-3 hydrogel and virgin hydrogel were tested (Fig. 2d). The fracture stress of the as-prepared PAA-D-3 hydrogel is only 119 kPa, while that of the virgin PAA-D-3 hydrogel reaches 395 kPa, which is nearly 3 times higher than that of the as-prepared hydrogel, and maintains a high fracture strain. The improvement in the mechanical properties from the as-prepared PAA-D-3 hydrogel to the virgin hydrogel indicates that both an abundance of microdomain macrocrosslinkers and interchain complexes are formed during dialysis in water [21].

Self-healing behavior of the PAA-D-n hydrogels

To investigate the recovery of the PAAc/DETA hydrogels, cyclic recovery tests with different waiting times were conducted, as shown in Fig. 3a. The waiting time dependences of the residual strain and the hysteresis ratio estimated from the hysteresis area change (Fig. 3b) present a two-stage recovery. After the first stretch, the PAA-D-3 hydrogel is able to restore most of the original stiffness after 1 minute in the first stage; however, plastic deformation is not able to be rapidly and completely removed upon

increasing the waiting time in the second stage. The hysteresis area enclosed by the first loading–unloading cycle is up to 50% of the overall area below the loading curve (work of extension) and finally recovers to approximately 65%. However, the sample still shows a 35% residual energy, indicating that the strong ionic bonds between the secondary amino group and carboxylic acid group are broken at 600% strain, and these bonds take longer to reform in the network of PAAc [30]. The proposed recovery mechanism is shown in Fig. 3c. During the loading cycle, both the weak ionic bonds (between carboxylate and the primary ammonium ions) and the single strong ionic bond (between carboxylate and the secondary ammonium ions) are broken; however, only the two weak ionic bonds can be restored quickly during the unloading cycle, while the strong bonds require a longer time to fully reform.

The step shear measurements of the PAA-D-3 hydrogel under periodic 100 and 20% shear were conducted to test the self-healing properties of the PAAc/DETA hydrogels (Fig. 4a). The G′ value of the PAA-D-3 hydrogel is one order of magnitude larger than that of the G″ value under 20% shear, indicating the formation of a self-standing hydrogel; however, the inverted G′ and G″ values under
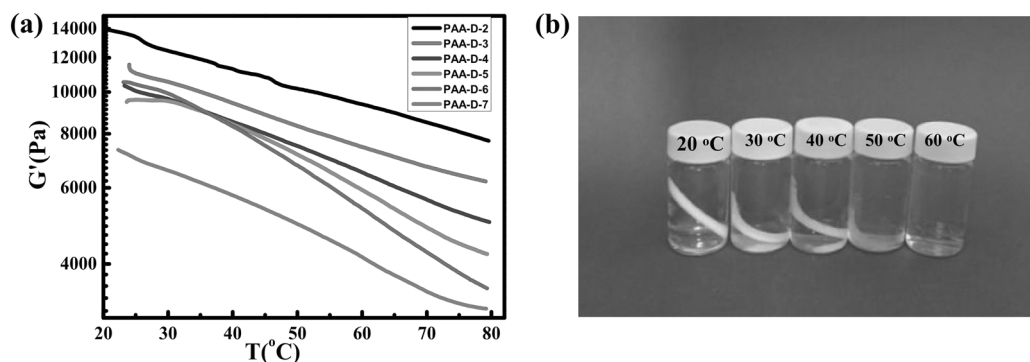
Fig. 5 a Elastic modulus, G′, of the PAA-D-n hydrogels plotted as a function of temperature. **b** Transition of the transparency of the PAA-D-7 hydrogel at different temperatures

Fig. 6 The shape memory behavior of the PAA-D-7 hydrogel with a specific shape as shown in (**a**) permanent shape, (**b**) temporary shape, and immersing the hydrogel in a water bath at 60 °C for (**c**) t = 2 s, (**d**) t = 5 s and (**e**) t = 30 s
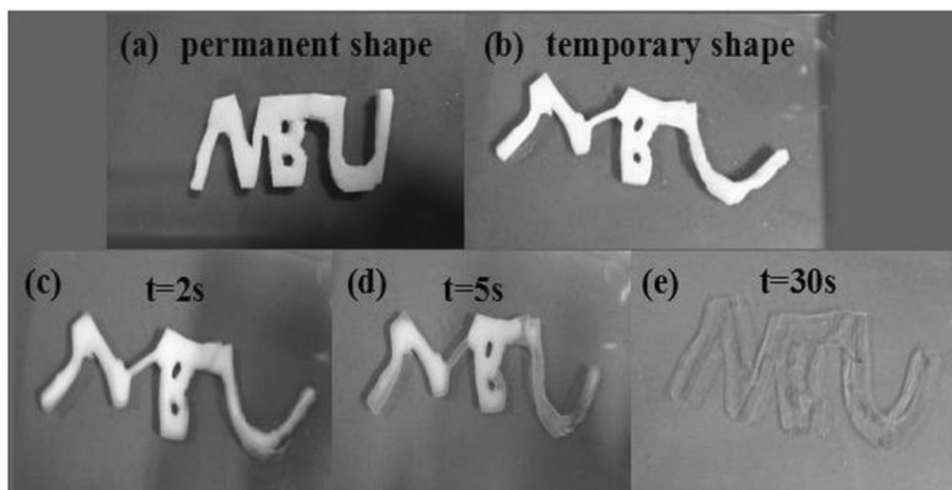


100% shear indicate that the internal structure of the hydrogel is destroyed under shear stress. A total of 63% of the G′ value is restored under 20% shear due to the reversible formation of microdomains and part of the ionic bonds that provide the self-healing feature of hydrogels. As shown in Fig. 4b, the cylindrical samples were cut into two pieces, and one of them was stained with rhodamine to distinguish the two pieces easily. Then, the cut surfaces were brought together to form a contact, sealed in a syringe and left to stand for 24 h in the ambient conditions. The cut samples heal well and withstand a weight of 100 g. The stiffness of the self-healed hydrogel was tested for comparison with that of the virgin hydrogel (Fig. 4c). The healed PAA-D-3 hydrogel sample sustains a 258 kPa stress, ruptures at a stretch of 933% and can maintain 68% of the original fracture energy (Fig. 4d).

Shape memory behavior of the PAA-D-n hydrogels

Because of the temperature-related reversible ionization, oscillatory temperature sweep experiments were performed to study the influence of the temperature on the rheological properties of the PAA-D-n hydrogels (Fig. 5a). A decrease in the elastic modulus upon increasing the temperature is observed. Such a large difference in the modulus between high and low temperatures is the most significant factor for inducing the shape memory effect [22]. In addition to the mechanical properties, the transparency of the hydrogels is also sensitive to the temperature. For instance, the PAA-D-7 hydrogel exhibits a white opaque state at 25 °C; when the temperature is increased to 40 °C, the hydrogel transforms into a fuzzy translucent state; the hydrogel becomes completely colorless and transparent when the temperature is 60 °C (Fig. 5b). This result indicates that the two-phase structure of the hydrogel becomes homogeneous with increasing temperature, which can be attributed to disassociation of the hydrophobic domains, as observed in the NMR experiments.

The PAAc/DETA hydrogel was utilized to investigate the thermally activated shape memory effect. The photos in Fig. 6 show the thermoresponsive shape memory behavior of the PAA-D-7 hydrogel. The permanent shape of the sample forms the letters NBU, the abbreviated name of our university (Fig. 6a). After heating to 60 °C, the hydrogel becomes soft and can be deformed into a temporary shape
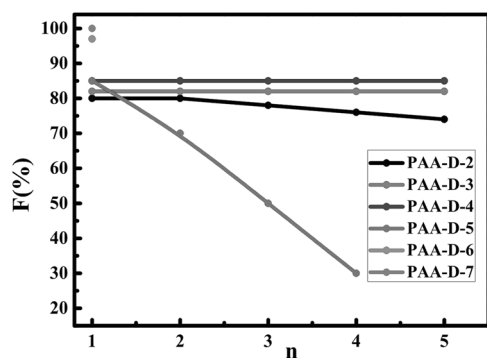
Fig. 7 Repeatability of the shape fixing efficiencies of the PAA-D-n hydrogels

(Fig. 6b). The temporary shape is fixed by cooling the sample to 25 °C. After immersing the hydrogel in a water bath at 60 °C, it returns to its initial shape within one minute (Fig. 6c,). The mechanism of temperature-sensitive shape memory can be attributed to the noncovalent crosslinks formed from ionic bonding and hydrophobic interactions to lock the hydrogel in a temporary shape. When the hydrogel is heated to 60 °C, the physical microdomains crosslinked by PAAc and DETA successively dissociate, and the sample can be easily deformed. After being cooled to room temperature, the physical crosslinks form again to fix the shape. The initial shape can be recovered by dissociating the microdomains, and thus, the transition from the white opaque state to the transparent state is also observed (Fig. 6e).

The repeatability of the shape-fixing efficiency, *F*, was calculated according to the previously reported method [23], as shown in Fig. 7. In the first cycle, all of the PAA-D-n hydrogels exhibit an 80–100% fixing efficiency; however, the PAA-D-6 and PAA-D-7 hydrogels become brittle in the second cycle. For PAA-D-5, the hydrogel show an 85% fixing efficiency in the first cycle, while the efficiency decreases to 70% in the second cycle and 32% in the fourth cycle. On the other hand, for $n = 3, 4$, the fixing efficiency keeps constant at proximately 85%, even in the fifth cycle. For the shape memory hydrogels reported by Osada et al., [31, 32] the alkyl side chains of the polymers are in the crystalline state after cooling below the transition temperature, so the deformed shapes can be fixed. In the present system, the hydrophobic microdomains provide the shape fixing ability; therefore, the repeatable high shape-fixing efficiency requires a higher content of the PAAc/DETA complex in the hydrogel.

Conclusions

In the present work, we described a promising method for preparing self-healing hydrogels with shape memory behavior, as well as a high fracture energy (196 KJ m^{-3}) and stretch at break (1100%). Ionic bonds and

microdomains were formed between DETA and the PAAc chains in situ, after which dialysis in water was performed to extract the excess ions and DETA. The hydrogels equilibrated in water exhibited much better mechanical strengths than the as-prepared hydrogels. Cyclic tensile recovery tests conducted on the hydrogels showed good hysteresis, demonstrating that the damage to the hydrogel network was recoverable. The hydrogel samples that were self-healed in ambient conditions withstood stresses of up to 258 kPa and ruptured at a stretch of 933%. They also exhibited repeatable temperature-sensitive shape memory properties. The use of a commercially available small amine molecule and a polyelectrolyte to prepare self-healing materials provides great promise for the creation of novel, smart materials in which the mechanical properties can be tuned by adjusting the molar ratio. This synthetic strategy can also be extended to a wide variety of specific small molecules that interact with polymers to create materials with versatile functionalities.

Compliance with ethical standards

Conflict of interest The authors declare that they have no conflict of interest.

References

1. Wu DY, Meure S, Solomon D. Self-healing polymeric materials: a review of recent developments. Prog Polym Sci. 2008;33:479–522.
2. Yang Y, Urban MW. Self-healing polymeric materials. Chem Soc Rev. 2013;42:7446–67.
3. Herbst F, Döhler D, Michael P, Binder WH. Self-healing polymers via supramolecular forces. Macromol Rapid Commun. 2013;34:203–20.
4. Taylor DL, in het Panhuis M. Self-healing hydrogels. Adv Mater. 2016;28:9060–93.
5. Phadke A, Zhang C, Arman B, Hsu C-C, Mashelkar RA, Lele AK, Tauber MJ, Arya G, Varghese S. Rapid self-healing hydrogels. Proc Natl Acad Sci. 2012;109:4383–8.
6. Li L, Yan B, Yang J, Chen L, Zeng H. Novel mussel-inspired injectable self-healing hydrogel with anti-biofouling property. Adv Mater. 2015;27:1294–9.
7. Nakahata M, Takashima Y, Yamaguchi H, Harada A. Redox-responsive self-healing materials formed from host–guest polymers. Nat Commun. 2011;2:511.
8. Xu Y, Wu Q, Sun Y, Bai H, Shi G. Three-dimensional self-assembly of graphene oxide and dna into multifunctional hydrogels. ACS Nano. 2010;4:7358–62.
9. Huebsch N, Kearney CJ, Zhao X, Kim J, Cezar CA, Suo Z, Mooney DJ. Ultrasound-triggered disruption and self-healing of reversibly cross-linked hydrogels for drug delivery and enhanced chemotherapy. Proc Natl Acad Sci. 2014;111:9762–7.

10. Tseng T-C, Tao L, Hsieh F-Y, Wei Y, Chiu I-M, Hsu S-H. An injectable, self-healing hydrogel to repair the central nervous system. Adv Mater. 2015;27:3518–24.

11. Cui J, Campo AD. Multivalent H-bonds for self-healing hydrogels. Chem Commun. 2012;48:9302–4.

12. Chen C, Wu D, Fu W, Li Z. Peptide hydrogels assembled from nonionic alkyl-polypeptide amphiphiles prepared by ring-opening polymerization. Biomacromolecules. 2013;14:2494–8.

13. Krogsgaard M, Behrens MA, Pedersen JS, Birkedal H. Self-healing mussel-inspired multi-ph-responsive hydrogels. Biomacromolecules. 2013;14:297–301.

14. Kakuta T, Takashima Y, Nakahata M, Otsubo M, Yamaguchi H, Harada A. Preorganized hydrogel: self-healing properties of supramolecular hydrogels formed by polymerization of host–guest-monomers that contain cyclodextrins and hydrophobic guest groups. Adv Mater. 2013;25:2849–53.

15. Miyamae K, Nakahata M, Takashima Y, Harada A. Self-healing, expansion–contraction, and shape-memory properties of a pre-organized supramolecular hydrogel through host–guest interactions. Angew Chem Int Ed. 2015;54:8984–7.

16. Tomatsu I, Hashidzume A, Harada A. Redox-responsive hydrogel system using the molecular recognition of β-cyclodextrin. Macromol Rapid Commun. 2006;27:238–41.

17. Tuncaboylu DC, Sari M, Oppermann W, Okay O. Tough and self-healing hydrogels formed via hydrophobic interactions. Macromolecules. 2011;44:4997–5005.

18. Wang Q, Mynar JL, Yoshida M, Lee E, Lee M, Okuro K, Kinbara K, Aida T. High-water-content mouldable hydrogels by mixing clay and a dendritic molecular binder. Nature. 2010;463:339–43.

19. Sun TL, Kurokawa T, Kuroda S, Ihsan AB, Akasaki T, Sato K, Haque MA, Nakajima T, Gong JP. Physical hydrogels composed of polyampholytes demonstrate high toughness and viscoelasticity. Nat Mater. 2013;12:932–7.

20. Haraguchi K, Uyama K, Tanimoto H. Self-healing in nanocomposite hydrogels. Macromol Rapid Commun. 2011;32:1253–8.

21. Luo F, Sun TL, Nakajima T, Kurokawa T, Zhao Y, Sato K, Ihsan AB, Li X, Guo H, Gong JP. Oppositely charged polyelectrolytes form tough, self-healing, and rebuildable hydrogels. Adv Mater. 2015;27:2722–7.

22. Gulyuz U, Okay O. Self-healing poly(acrylic acid) hydrogels with shape memory behavior of high mechanical strength. Macromolecules. 2014;47:6889–99.

23. Hao J, Weiss RA. Mechanically tough, thermally activated shape memory hydrogels. Acs Macro Lett. 2013;2:86–9.

24. Yu J, Chuang SSC. The structure of adsorbed species on immobilized amines in CO2 capture: an in situ ir study. Energy Fuels. 2016;30:7579–87.

25. Moon D, Tanaka S, Akitsu T, Choi J-H. Molecular structure, spectroscopic properties, and Hirshfeld surface analysis of chlorobis(N-methyl-1,3-propanediamine)copper(II) tetrafluoroborate and azidobis(2,2-dimethyl-1,3-propanediamine)copper(II) azide. J Mol Struct. 2018;1154:338–47.

26. Hu J, Hiwatashi K, Kurokawa T, Liang SM, Wu ZL, Gong JP. Microgel-reinforced hydrogel films with high mechanical strength and their visible mesoscale fracture structure. Macromolecules. 2011;44:7775–81.

27. Sun Y, Gao G, Du G, Cheng Y, Fu J. Super tough, ultrastretchable, and thermoresponsive hydrogels with functionalized triblock copolymer micelles as macro-cross-linkers. Acs Macro Lett. 2014;3:496–500.

28. Yuan N, Xu L, Wang H, Fu Y, Zhang Z, Liu L, Wang C, Zhao J, Rong J. Dual physically cross-linked double network hydrogels with high mechanical strength, fatigue resistance, notch-insensitivity, and self-healing properties. ACS Appl Mater Interfaces. 2016;8:34034–44.

29. Rumyantsev AM, Pan A, Ghosh Roy S, De P, Kramarenko EY. Polyelectrolyte gel swelling and conductivity vs counterion type, cross-linking density, and solvent polarity. Macromolecules. 2016;49:6630–43.

30. Luo F, Sun TL, Nakajima T, Kurokawa T, Li X, Guo H, Huang Y, Zhang H, Gong JP. Tough polyion-complex hydrogels from soft to stiff controlled by monomer structure. Polymer. 2017;116:487–97.

31. Tanaka Y, Kagami Y, Matsuda A, Osada Y. Thermoreversible transition of tensile modulus of hydrogel with ordered aggregates. Macromolecules. 1995;28:2574–6.

32. Osada Y, Matsuda A. Shape memory in hydrogels. Nature. 1995;376:219.